ROYAL SOCIETY OF CHEMISTRY

An investigation of free-energy-averaged (coarse-grained) potentials for fluid adsorption on heterogeneous solid surfaces

Srikanth Ravipati[ab], Amparo Galindo[ab], George Jackson[ab] and Andrew J. Haslam[*ab]

Coarse-grained, two-body fluid–solid potentials provide a simple way to describe the interaction between a fluid molecule and a solid surface in adsorption theories, and also a means to reduce the computational expense in molecular simulations, compared to those employing full atomistic detail. Here we investigate the applicability of a recently proposed mapping procedure to obtain free-energy-averaged (FEA) fluid–solid interactions for fluids on various heterogeneous surfaces. Methane and graphite (respectively) are chosen as the fluid and the solid, and the surface graphene layer is modified to create chemical and geometrical heterogeneities; for the latter surfaces, the FEA mapping is appropriately modified to account for vacancies. Adsorption isotherms and fluid density profiles are obtained by performing grand canonical Monte Carlo (GCMC) simulations for explicit-solid and FEA-potential representations, and are compared to gain insights about the applicability and limitations of the FEA potentials. For solids with homogeneous and chemically heterogeneous surfaces, adsorption isotherms and density profiles obtained using FEA potentials are in good agreement with those obtained using an explicit-solid representation. For surfaces containing vacancies, isotherms and density profiles obtained using the unmodified FEA potential differ significantly from their explicit-surface analogues. When using the FEA potential obtained via the modified mapping procedure some deviations are still seen at very high pressure however, at low to moderate pressures, agreement is, once again, good.

1 Introduction

Fluid adsorption, wetting, and capillary condensation involving fluid–solid interfaces are important phenomena in many processes both in nature and in industry. In studies of fluid–solid interfaces, an implicit assumption that the solid surface is homogeneous is very common. Solids with homogeneous surfaces are used in many molecular-simulation and theoretical studies to investigate and understand the fluid behaviour at fluid–solid interfaces. In reality, however, either in nature or industrial applications, solid surfaces are heterogeneous and thus understanding fluid interaction with such surfaces is of great interest.

Characterizing adsorbent surface chemical heterogeneity and its influence on fluid adsorption has been studied by treating the solid surface as a distribution of patches[?,?,?]; in this approach a different energy of adsorption for the fluid is assigned to each patch. The overall measure of adsorption, θ_t, is made up of local contributions, θ_l, from the individual patches and is given by

$$\theta_{t,U}(P,T) = \int \theta_l(U,P,T)\mathscr{P}(U)dU, \qquad (1)$$

where P and T are the pressure and absolute temperature, U is the fluid–solid interaction energy, and $\mathscr{P}(U)$ is the probability distribution of the energy of adsorption. Typically, a parameterised analytical form is assumed *a priori* for the distribution, and the unknown parameters are regressed using the experimental adsorption isotherm.

Despite its widespread use, this approach is strictly applicable only for the case of chemically heterogeneous surfaces (*i.e.*, surfaces containing defect (or hetero-) atoms). Another class of surface heterogeneity is that characterised by the presence of vacancies, or surface roughness. To model these systems, different degrees of surface roughness can be accommodated by considering a smooth surface but in pores of varying widths; the effect of the heterogeneity is thereby transferred from the surface itself into a distribution of pore widths. Within this framework, eq. (1)

[a] Molecular Systems Engineering, Department of Chemical Engineering, Imperial College London, London SW7 2AZ, UK. E-mail: g.jackson@imperial.ac.uk
[b] Qatar Carbonates and Carbon Storage Research Centre (QCCSRC), Department of Chemical Engineering, Imperial College London, London SW7 2AZ, UK

is recast in the following form:

$$\theta_{t,H}(P,T) = \int \theta_l(H,P,T)\mathscr{P}(H)dH; \qquad (2)$$

here $\theta_l(H,P,T)$ is the local isotherm at a pore width of H and $\mathscr{P}(H)$ is the probability distribution of pore widths, generally referred to as the pore-size distribution (PSD). PSDs are optimised to match experimental isotherms using isotherms corresponding to homogeneous surfaces of different pore widths according to $\mathscr{P}(H)$. To model rough surfaces with chemical heterogeneities an equation analogous to eq. (1) and eq. (2), in which the distribution is a function of both energy and pore width, was adopted by [?].[?]

Non-local density functional theory (NL-DFT)[????] can be used to obtain the local isotherms required in eqs. (1) and (2). For example, NL-DFT has been successfully used to obtain adsorption isotherms corresponding to different pore widths as required in eq. (2) to obtain an overall measure of adsorption. However, adsorption isotherms thus obtained using NL-DFT for porous solids with heterogeneous surfaces exhibited multi-step layer transitions that are exclusive to homogeneous surfaces, and were not seen in the isotherms from experiments.

Molecular simulations were used to understand the adsorption behaviour on different heterogeneous surfaces; adsorption isotherms from simulations of heterogeneous surfaces were qualitatively similar to the isotherms from experiments, without the presence of multi-step layer transitions.[????????] Insights from these simulation studies led to the conclusion that the use of isotherms obtained using homogeneous surfaces of different pore widths in eq. (2) had given rise to artificial gaps in the PSD and the multi-step layer transition.

More recently, quenched-solid density functional theory (QS-DFT)[???] was proposed, in which one assumes a diffuse solid wall at the fluid–solid interface. Modeling the fluid–solid interface as diffuse, in the case of surfaces with vacancies, eliminated the layering transitions in the theoretical isotherms and led to good agreement with the experiments. Two-dimensional (2D)-NL-DFT that can accommodate lateral structural details showed improvement over the NL-DFT, but at a higher computational cost. Subsequently, [?] and [?] proposed random-surface density functional theory (RS-DFT) based on the theory of random processes to model rough surfaces. The hybrid reverse Monte Carlo technique[????] was also used to generate realistic molecular models of micro-porous carbon structures utilizing experimental scattering data.

Although molecular simulations (such as molecular dynamics, GCMC and hybrid reverse Monte Carlo) provide direct insights into the detailed nature of the PSD, the computational cost is high. An alternative is to use the theoretical approaches such as statistical associating fluid theory (SAFT)[??], other adsorption theories based on a variety of equation of states[??] and density-functional theory (DFT)[????] in the context of adsorption, but

potential, which can be used to represent the interaction between an LJ fluid and a mono-layer, and the LJ 10-4 potential, for the interaction with a multi-layered LJ solid.[?] [?] developed the 10-4-3 coarse-grained potential to better represent the LJ-fluid interaction with a multi-layered LJ solid.

It has long been established that coarse-grained potentials, in which one averages out variables that are not of interest, should contain an appropriate temperature dependence in order that the free energy of the coarse-grained system does not differ from that of the system described in full (explicit) detail.[?????????]. Although the LJ 9-3 and 10-4, and Steele 10-4-3 potentials have been used with great success over a number of years, they nevertheless suffer a limitation insofar as they contain no such temperature dependence. In certain circumstances, such as systems featuring surfaces with widely spaced atoms or containing defects, this deficiency can lead to discernibly different thermodynamic properties; notably it can lead to different adsorption isotherms. To circumvent this, a rigorous free-energy-averaged (FEA) mapping was recently proposed to coarse-grain the fluid–solid potentials.[?] The FEA mapping naturally yields an appropriate temperature dependence and, reflecting this, fluid isotherms obtained using a FEA potential were shown to be in good agreement with those obtained using the explicit-solid representation, for homogeneous and chemically heterogeneous surfaces.

Following the same theme, in our current work we seek to further our understanding of the use of FEA potentials in adsorption calculations. In particular, we investigate the applicability of FEA potentials for fluid–surface interactions relating to solid surfaces with random chemical and geometric heterogeneities. The FEA mapping procedure is appropriately modified to account for vacancies in geometrically heterogeneous surfaces. Fluid adsorption isotherms and density profiles obtained using the resulting FEA potentials are compared to those obtained using the explicit-solid representation.

This paper is set out as follows: in section 2 we set out the theoretical background to our work, and discuss its computational implementation. The results of the work are set out in section 3. Finally, in section 4, we summarise and discuss our findings, and present our conclusions.

2 Methodology

2.1 Free energy mapping

For a system of a single fluid molecule interacting with a solid, with atoms fixed to their lattice positions, the partition function is given by[?]

$$Q(D) = F_f(T)\mathscr{A}_s(D)\langle \exp[-\beta U_{fs}]\rangle_{(x_f,y_f,z_f=D)}; \qquad (3)$$

here T is the temperature, $\beta = 1/(k_B T)$, k_B is the Boltzmann constant, $F_f(T)$ represents the kinetic degrees of freedom of the fluid molecule, and $\mathscr{A}_s(D)$ is the solid surface area available for the fluid. U_{fs} is the total fluid–solid intermolecular potential, result-

(See Ref.[?] for details.)

In the coarse-grained (CG) description, the fluid molecule interacts with a featureless (structureless) solid. The partition function is then given by

$$Q_{CG}(D) = F_f(T) \mathscr{A}_{s,CG}(D) \exp\left[-\beta \mathscr{W}(D)\right], \quad (4)$$

where $\mathscr{W}(D)$ is the interaction of the fluid molecule with the solid, at a distance D from the surface. $\mathscr{A}_{s,CG}(D)$ is the surface area available for the fluid in the CG description.

In this description, the fluid–solid interaction depends only on the normal distance of the fluid molecule from the solid surface and is independent of the lateral position of the fluid molecule.

The FEA mapping of the fluid interaction with explicit solid onto the CG description is implemented by equating the free-energies (or equivalently the partition functions, given in equations 3 and 4, i.e., $Q(D) = Q_{CG}(D)$), and this results in the CG description of the fluid–solid interaction,

$$\mathscr{W}(D) = -\frac{1}{\beta} \ln\left(\frac{\mathscr{A}_s(D)}{\mathscr{A}_{s,CG}(D)} \langle \exp\left[-\beta U(D)\right]\rangle\right). \quad (5)$$

For convenience, we introduce a new quantity, $\overline{f_{\mathscr{A}}}(D)$, defined as

$$\overline{f_{\mathscr{A}}}(D) = \mathscr{A}_s(D)/\mathscr{A}_{s,CG}(D); \quad (6)$$

the computation of this quantity is explained in the following subsection.

Note that the distance D is always measured from the uppermost vacancy-free layer. If the solid surface contains vacancies, the distance of a fluid molecule from the solid surface (D) is thus not measured from the top surface layer (which contains the vacancies). In our study, only the first surface layer contains vacancies, and D is thus measured from the second layer.

For the limiting case of a solid with a vacancy-free surface, $\overline{f_{\mathscr{A}}}(D) = 1$, whereby equation 5 becomes

$$\mathscr{W}_{vf}(D) = -\frac{1}{\beta} \ln\langle\exp\left[-\beta U(D)\right]\rangle, \quad (7)$$

where the subscript "vf" denotes "vacancy free".

2.1.1 Computational implementation

All the volume available to the fluid is discretised into planar bins, categorised in terms of D. In each bin, a large number of fluid-molecule trial insertions are performed to probe the whole lateral area parallel to the surface. For each insertion, D is recorded and U_{sf} is computed to obtain the average $\langle\exp\left[-\beta U(D)\right]\rangle$ required in eq. (7) or eq. (5). In the presence of vacancies in the solid surface, $\overline{f_{\mathscr{A}}}(D)$ is also estimated as the ratio of number of non-overlapping fluid molecule insertions to the total number of attempted trail insertions. The probe fluid molecule is considered to be overlapping if $r_{sf} < 0.8\sigma_{sf}$, where r_{sf} is the distance between the fluid and solid molecule and σ_{sf} is the fluid–solid core diameter (see section 2.3).

2.2 System of study

Our choice of model system is based largely on convenience and simplicity, while retaining some representation of a realistic system. Graphite (with five layers of graphene) is chosen as the solid substrate, with methane selected as the adsorbing fluid; "off-the-shelf" potentials are adopted for both carbon and methane. Different types of heterogeneities are modelled by modifying the surface layer. We consider four different surfaces:

- a homogeneous surface;

- a chemically heterogeneous surface;

- a geometrically heterogeneous surface;

and

- a surface with both chemical and geometric heterogeneities.

A chemically heterogeneous surface is modelled by modifying the methane–solid-substrate carbon atom interaction for one or more surface-layer carbon atoms; from the point of view of the adsorbing fluid, such carbon atoms thereby become heteroatoms. A geometrically heterogeneous surface is modelled by deleting one or more carbon atoms from the surface graphene layer, thereby introducing surface roughness.

2.3 Force-field and simulation details

Methane is modelled as a single-site molecule using the TraPPE forcefield[?]. Interactions among carbon atoms in graphene are modeled using a LJ potential; the potential parameters are taken from [?]. Unlike (cross) interaction parameters are obtained using the Lorentz-Berthelot rules, i.e., $\sigma_{sf} = (\sigma_{ff} + \sigma_{ss})/2$ and $\varepsilon_{sf} = (\varepsilon_{ff}\varepsilon_{ss})^{1/2}$. All the interaction parameters used in this study are provided in table 1. The lateral dimensions of the solid as well as the simulation box are 31.980 Å × 34.087 Å and each (vacancy-free) graphene layer contains 416 carbon atoms. In adsorption simulations and FEA potential computations, periodicity is adopted in the lateral (x and y) directions, while solid is placed at both extremes in the z-direction (which, thereby, is non-periodic). In practice, however, we find that computational efficiency is improved by replacing one of the solid boundaries with a hard wall; provided that the length (z-dimension) is sufficiently large we find that adsorption characteristics with the solid are unaffected. (In this case analysis is, of course, limited to the interaction of the fluid with the (graphite) solid only.) The length of the simulation box in the z-direction is 43.2 Å. All the interactions are cut off at a separation of 12.0 Å; no tail corrections are employed.

To obtain the FEA potential, eq. (7), the fluid volume in the direction normal to the solid is discretised in bin widths of 1 Å, and for each bin 5×10^6 trial insertions of fluid molecules are attempted. For each insertion, $U(D)$ is computed, and the FEA potential, $\mathscr{W}(D)$ is latterly accumulated according to equation 5. For surfaces containing vacancies, we also record whether or not the

A Chebyshev representation is chosen since this allows for an essentially perfect continuous description even of quite complicated functions however, where appropriate, we also consider approximate descriptions using the more-compact Mie-potential form.

Adsorption isotherms are obtained by performing simulations in the grand-canonical ensemble, *i.e.*, at fixed chemical potential (μ), volume (V) and temperature (T). All the simulations are performed at $T = 273$ K. Complementary (μ, V, T) simulations are performed for bulk fluid at the same thermodynamic conditions (*i.e.*, with no solid, and with full 3-D periodicity) to provide correspondence between the confined and bulk fluid. The pressure of the bulk fluid is then obtained by further simulation in the canonical (N, V, T) ensemble, at the corresponding bulk-fluid density, using the test-volume perturbation approach[?][?][?][?]. All the simulations consist of 50000 equilibrium cycles and 50000 production cycles, with each cycle comprising 200 Monte Carlo (MC) moves. In (N, V, T) simulations, translation is the only MC move, whereas in (μ, V, T) simulations insertion and deletion moves are also carried out; each class of MC move is chosen with equal probability. Note that the error bars in the figures in the following section correspond to standard errors computed by dividing the production stage into four blocks, as described in section 8.4 of the book of Allen and Tildesley[?].

3 Results and discussion

Fluid adsorption isotherm and density profiles are obtained by performing (μ, V, T) simulations for both explicit-solid and FEA potential representations, and are compared for the different solid surfaces considered in the study.

3.1 Methane on homogeneous graphene

We start with the system of methane adsorbing on a graphite substrate with a homogeneous surface; the surface layer is illustrated in fig. 1. The FEA potential obtained using eq. (7) and its fitted continuous representation are shown in fig. 2.

The adsorption isotherm obtained using the FEA potential is in good agreement with the one obtained using the explicit-solid representation (fig. 3), as shown previously by [?]. In addition, the fluid density profile obtained using the FEA potential is also in good agreement with that obtained using the explicit-solid representation, as can be seen in fig. 5. (Note that in this, and subsequent figures depicting density profiles, although the profiles relating to the explicit-solid and CG descriptions are obtained in identical fashion, for clarity, that relating to the explicit description is plotted using a curve while that relating to the CG description is indicated with symbols. Note also that the density is defined in terms of the average number of molecules (obtained from (μ, V, T) simulations) and a scaling volume defined to be the volume available to the fluid in the case where the solid has no vacancies.)

The analytical forms and coefficients of the Chebyshev representation

tential form, as demonstrated by [?]. The Mie form is given by

$$u_{\text{fs}}^{\text{Mie}}(D) = \mathscr{C}\varepsilon\left[\left(\frac{\sigma}{D}\right)^{\lambda_r} - \left(\frac{\sigma}{D}\right)^{\lambda_a}\right] \qquad (8)$$

where $u_{\text{fs}}(D)$ is the interaction of a fluid molecule at a distance of D from the CG solid surface, ε is the potential depth, σ is the hard-core diameter between fluid molecule and the CG surface, λ_r and λ_a are the repulsive and attractive exponents in the Mie potential, and $\mathscr{C} = \frac{\lambda_r}{(\lambda_r - \lambda_a)}\left(\frac{\lambda_r}{\lambda_a}\right)^{\frac{\lambda_a}{(\lambda_r - \lambda_a)}}$. The parameter values of the Mie potentials regressed to FEA potentials of methane interacting with homogeneous graphene surfaces are $\varepsilon/(k_B T) = 4.723$ K, $\sigma = 3.027$ Å, $\lambda_r = 8.121$, and $\lambda_a = 4.629$.
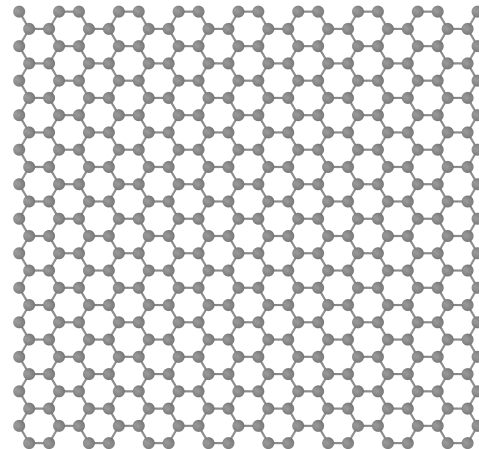

Fig. 1 Homogeneous graphene surface.

3.2 Methane on chemically heterogeneous graphene

Chemical heterogeneities are modelled by introducing defect (or hetero-) atoms; interactions of the fluid molecules with some carbon atoms of the surface graphene layer are modified (parameters are given in table 1). We consider a system in which 166 of the atoms in fig. 1 become heteroatoms. The fluid–solid FEA potential obtained for this system (fig. 7) is qualitatively very similar to the case of graphite with a homogeneous surface. A comparison of FEA potentials obtained for methane on a homogeneous graphene surface (fig. 1), and a chemically heterogeneous surface (fig. 6) is shown in fig. 8. It is interesting to note in passing that the potential obtained for this heterogeneous surface is not well described using a simple Mie form.

Comparing the two FEA potentials displayed in fig. 8, relating to the homogeneous and chemically heterogenous surfaces, one can discern two noticeable differences in terms of potential depth and location at which potential minimum occurs. The magnitude of the potential depth increases corresponding to the increase in the depth of the methane–carbon atom interaction, and also the distance at which potential minimum occurs increases in accordance with the larger methane–carbon core diameter value (ta-

Table 1 Interaction parameters used in the study. Methane is modelled as a single-site molecule using the TraPPE forcefield[?]. Carbon atoms are modelled using the LJ potential with parameters from [?]. Defect carbon atoms are indicated using the letter "D".

Site1–Site2	(ε/k_B) / K	σ/ Å
CH_4–CH_4	148.00	3.730
C–C	28.000	3.400
CH_4–C	64.370	3.565
CH_4–D	143.94	4.070
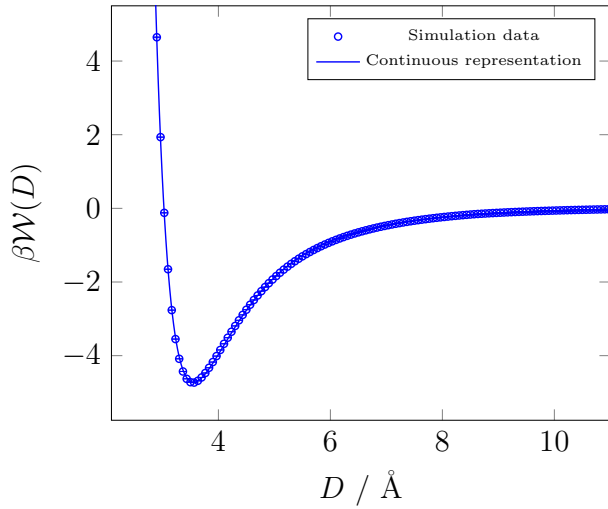
Fig. 2 The FEA potential of methane interacting with graphite of which the exposed graphene surface (fig. 1) is homogeneous. The symbols represent data obtained using eq. (7); the curve represents a fitted continuous representation of the data using a Mie form (note that this is visually indistinguishable from the representation obtained using a Chebyshev polynomial form).
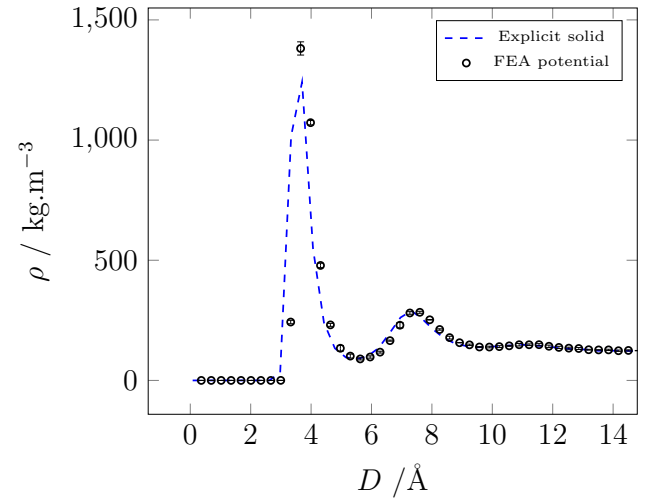
Fig. 3 Comparison of adsorption isotherms of methane on graphite of which the exposed graphene surface (fig. 1) is homogeneous. The

**Fig. 4** Density profile of methane adsorbed on graphite of which the exposed graphene surface (fig. 1) is homogeneous, at a bulk pressure of 0.01279 GPa. The dashed curve corresponds to data obtained using explicit solid; the circles correspond to the profile obtained using the FEA potential (fig. 2).
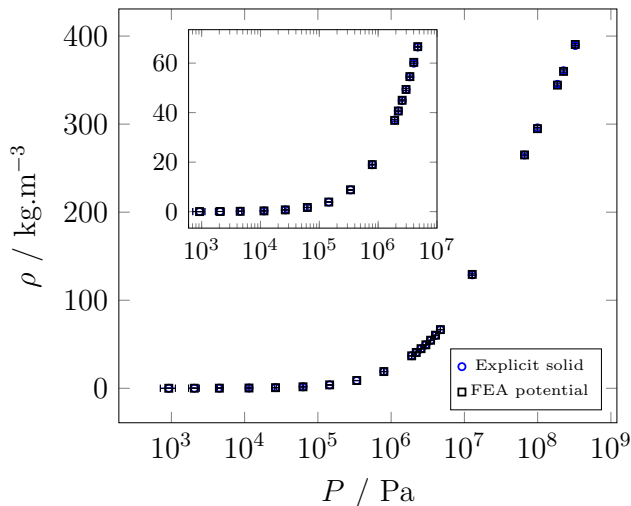
strated between the two isotherms obtained from these contrasting approaches.

3.3 Methane on geometrically heterogeneous graphene

A geometric heterogeneity is generated by deleting one or more carbon atoms from the surface graphene layer, thus creating surface vacancies. We report here results pertaining to the surface depicted in fig. 10, in which a total of 125 surface atoms have been removed. FEA potentials obtained for this system using eq. (7) and eq. (5) are shown in fig. 11. In addition to the FEA potentials, the fraction of the surface area available for the fluid $\overline{f_{\mathscr{A}}}(D)$, defined in eq. (6), is also shown in fig. 11. As discussed above, the fluid–solid distance, D, is measured from uppermost graphene layer that contains no vacancies, i.e., the second layer. $\overline{f_{\mathscr{A}}}(D)$ vs D has a smooth variation close to the fluid–solid interface, as seen in fig. 11. (In the case of a vacancy-free graphene surface, $\overline{f_{\mathscr{A}}}(D)$ vs D would be a step function reflecting absence of vacancies in the solid surface layer.) Both the CG potentials are characterised by a double minimum, with a local minimum at $D \approx 3$ Å, followed by a rise to a local maximum and a fall to the global minimum at $D \approx 7$ Å. It is quite evident, however, that the region with $D \lesssim 5$
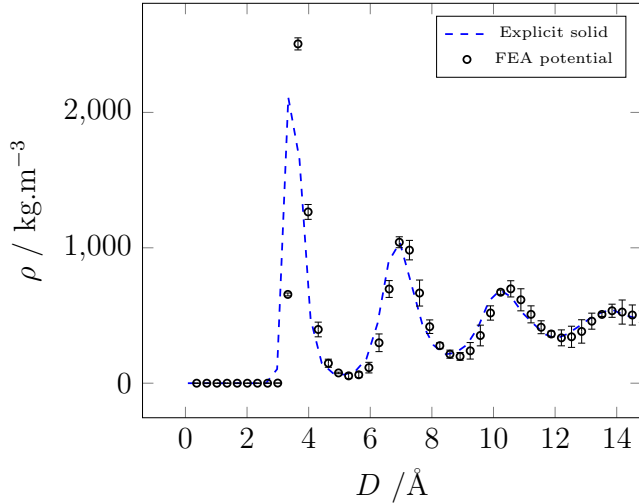
Fig. 5 The density profile of methane adsorbed on graphite of which the exposed graphene surface (fig. 1) is homogeneous, at a bulk pressure of 0.3265 GPa. The dashed curve corresponds to data obtained using explicit solid; the circles correspond to the profile obtained using the FEA potential (fig. 2).

Fig. 6 Chemically heterogeneous surface graphene layer. Those coloured in blue are (randomly selected) atoms for which the interaction with methane is modified (interaction-potential parameter values are given in table 1).

The temperature dependence of the FEA potentials is presented in fig. 15. At low temperature, the features of the potential are more pronounced. For example, the absolute values of the two minima in the potential decrease with increasing temperature. Indeed one sees that the local minimum at $D \sim 3.4$ Å gradually disappears; although not indicated in the figure, it "flattens" to a point of inflection at ~ 600 K, and becomes a shoulder at still higher temperatures. As another example, on close inspection, at the lower temperature of $T = 223$ K one can discern a small shoulder in the potential at $D \sim 6.4$ Å; no such shoulder is evident at higher temperatures.

For further analysis, we select a temperature of $T = 273$ K. For low to moderate pressures, the adsorption isotherm obtained using the FEA potential (eq. (5)) is in good agreement with that obtained using explicit solid, as can be seen in fig. 12. However, at high pressure, we observe discrepancies between isotherms from the two approaches. To better understand the origin of these discrepancies, fluid density profiles obtained using both representations are compared at a moderate pressure, 0.01279 GPa (fig. 13), and at the highest pressure, 0.3265 GPa (fig. 14), considered in this study. The fluid density profile at bulk pressure 0.01279 GPa (fig. 13)) obtained using the FEA potential is in good agreement with the one obtained using explicit solid, excepting the first peak in the density profile. This first peak corresponds to fluid adsorption into the vacancies in the solid surface; its position corresponds the fluid-molecule–surface distance D at which the CG potentials in fig. 11 display local minima. The height of this peak is governed by the number of available vacancies, whereby it is lower than the second peak, which corresponds to adsorption across the whole surface. The first peak is signif-

resulting surface presented to (as yet unadsorbed) fluid molecules is modified as a result. This is particularly impactful in the case where vacancies are clustered together, such as in this instance (see fig. 10). For the explicit case, each successive fluid molecule adsorbing into a vacancy cluster modifies the relative attractiveness to further fluid molecules since there is a benefit to the system free energy from the interaction not only with the (solid) atoms in the surface layer but also from interactions with any atoms and molecules surrounding them laterally; for our particular system, as can be inferred from table 1, the system energy benefit is greater for each successive fluid molecule adsorbed. In simulations using the CG surface, there is nothing to account for this effect; adsorbing molecules will be spread out over the whole surface and, except when the pressure is very high, isolated (relatively speaking) from each other.
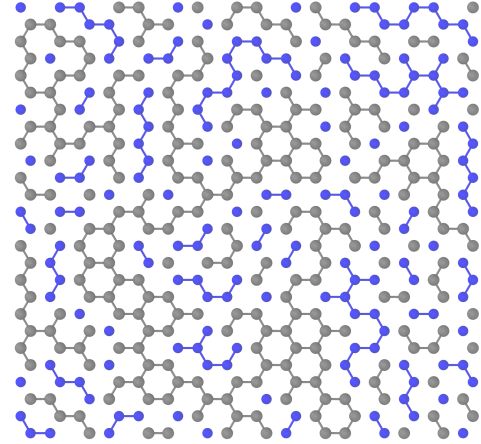
At very high bulk pressure, as can be seen in fig. 12, the fluid density obtained using the FEA potential is noticeably higher than the value obtained using explicit-solid case. The discrepancy in the total adsorption arises primarily from the first peak in the density profile. When the pressure is sufficiently high, fluid begins to adsorb significantly at the CG surface and, since the entire surface is available, more fluid molecules are able to adsorb than in the explicit-solid case, where adsorption is constrained by the number of vacancies that are available−as the density increases, successively fewer vacancies are available for adsorption in the surface layer until, at sufficiently high pressure, the vacancies are all filled. The first fluid density peak obtained using the FEA potential is therefore higher compared to that obtained using explicit solid, as can be seen in fig. 14 for the highest pressure considered, 0.3265 GPa; this contrasts the discrepancy observed at 0.01279 GPa bulk pressure (fig. 13), where the first peak, although similar for both simulations, is actually slightly higher for
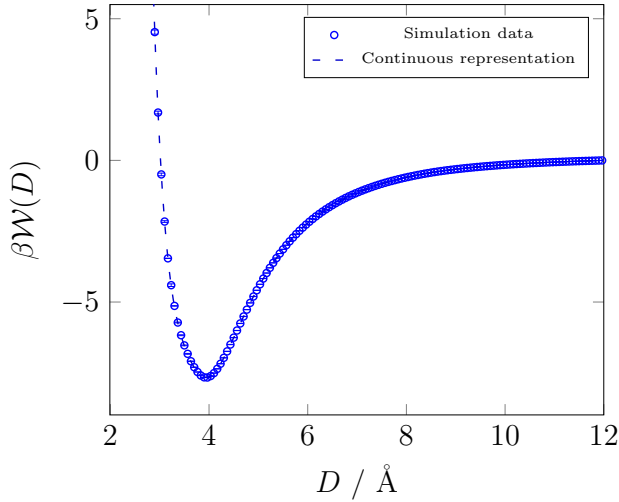
Fig. 7 The FEA potential of methane interacting with graphite of which the exposed surface (fig. 6) is chemically heterogeneous. The symbols represent data obtained using eq. (7); the dashed curve represents a continuous representation of these data (obtained using a so-called Chebyshev polynomial).
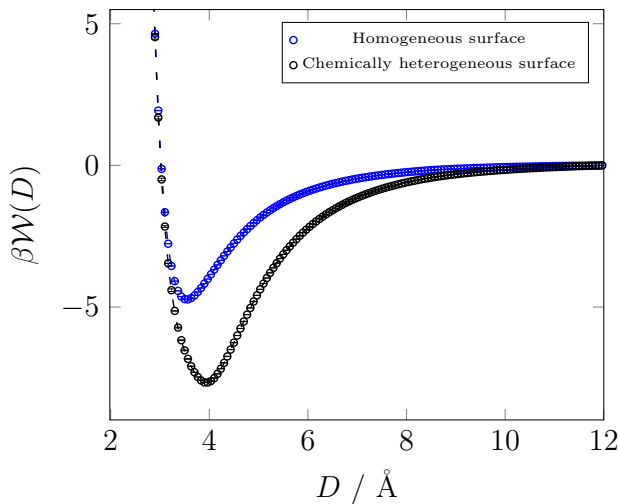

Fig. 8 Comparison of FEA potentials of methane interacting with graphite of which the exposed surface is homogeneous (fig. 1) and chemically heterogeneous (fig. 6). Dashed curves depict Chebyshev representations of the FEA potential data.
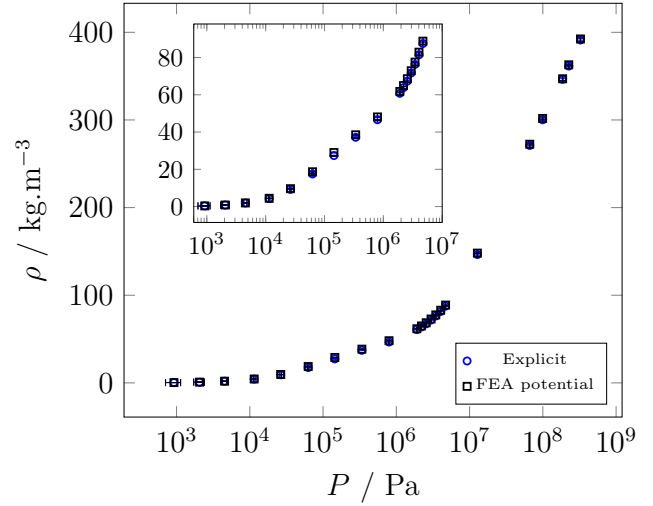
Fig. 9 Comparison of adsorption isotherms of methane on graphite of which the exposed surface (fig. 6) is chemically heterogeneous. The isotherm obtained using the FEA potential is indicated by the black squares; that obtained using explicit solid is indicated by the blue circles.

recently published work of which we became aware during the preparation of our manuscript. Shi *et al.*[?] followed a similar framework to address the CG potential for the case of fluid interacting with solid featuring a heterogeneous surface, although with subtle differences in implementation of the methodology; in brief these authors introduce a hard wall above the surface layer in the CG description and account for the vacancies in this hard wall (for details interested readers are referred to their article[?]). Our methodology leads to rather better agreement of fluid-density profiles (from the second adsorbed layer onwards); using our methodology this agreement persists even at high pressures, as can be seen in figures 13 and 14.

A limiting case of a geometrically heterogeneous surface modelled in this way was studied by [?], who examined an FCC LJ solid 111 surface with a single vacancy and LJ fluid; the FEA potential was obtained using eq. (7). Strictly speaking, as we have demonstrated in our current work, in the presence of vacancies in the solid surface the FEP potential should be obtained using eq. (5). However, for the case of a single vacancy within a large solid surface area, the difference between eq. (7) or eq. (5) is not expected to be significant.

A system such as ours, in the case where fluid is adsorbing onto explicit solid containing surface vacancies, can be thought of as featuring a diffuse solid–fluid interface. It is therefore interesting at this point to compare our work with that of [?] and [?]. To characterize porous carbon solids, these authors used non-graphitized carbon black (NGCB) with an amorphous surface layer as a reference solid in the DFT framework, instead of the more-commonly used graphitized carbon black with a homogeneous surface layer. [?] used NLDFT formulation and accounted for

distribution. **?** used an error function and **?** used a hyperbolic tangent function to model the diffuse nature of solid–fluid interface, taking inspiration from studies of the liquid–vapor interface. A parameter characterising the surface roughness was optimized so that calculated adsorption isotherms best described those determined experimentally. Both adsorption isotherms and fluid density profiles obtained in our current work are qualitatively similar to those obtained in these studies. In addition to the parameter corresponding to surface roughness, **?** also regressed the attractive part of the fluid–solid (one-body) potential and estimated the repulsive part from the excess free energy of the hard-sphere term. The fluid–solid potential obtained in our current work is qualitatively very similar to those obtained by **?**.

3.3.1 Porous substrate

So far, we have restricted our discussion to substrates with defects only in the surface graphene layer. An advantage of our coarse-graining approach is that it can be applied just as straightforwardly in the case that the defect characteristics of the substrate are far more complicated. For illustration, as a preliminary investigation, we compute the FEA potential of methane interacting with porous graphite, modelled by taking the geometrically heterogeneous substrate with surface-layer vacancies (see fig. 10) and introducing vacancies also into the second layer. The porous substrate thus generated is illustrated in fig. 16; we refer to this system as case II, while the simpler system with only surface-layer vacancies is here referred to as case I. The FEA potentials corresponding both cases are illustrated in fig. 17; note that, for comparative purposes, in plotting the potential corresponding to case I, D is here measured from the third graphene layer, rather than the second (as in fig. 11). The potential corresponding to case II incorporates some very interesting features, for example the introduction of the vacancies in the second layer leads to a local maximum in the curve, descending at shorter D (corresponding to second-layer vacancies) to a deep local minimum; this can be interpreted in the sense that the vacancies in the second graphene layer provide an attractive region to fluid molecules that is accessible by the fluid molecules only by overcoming a significant potential barrier; in this sense, the fluid molecules can be thought of as confined.

A more comprehensive investigation of fluid–solid systems featuring more-complex defect scenarios is ongoing, and will be presented in a future publication.

3.4 Methane on chemically and geometrically heterogeneous graphene

Finally, we consider a graphene surface containing both chemical and geometrical heterogeneites, incorporated as shown in fig. 18. The FEA potentials obtained for this system using eqs. (5) and (7) and also $\overline{f_{\mathscr{A}}}$ are shown in fig. 19 along with the continuous representation of the FEA potential obtained using eq. (5). The FEA potential for this case is qualitatively similar to the case of solid with
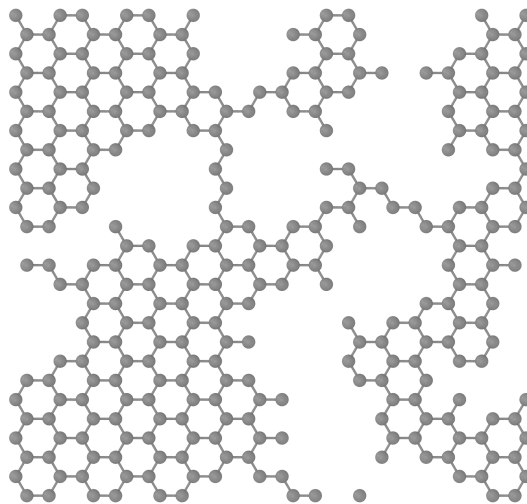

Fig. 10 Geometrically heterogeneous surface graphene layer. Geometric heterogeneities are represented by vacancies, generated by deleting randomly chosen carbon atoms from the surface graphene layer.

Insights from the comparison of adsorption isotherm and fluid density profiles for this case are similar to that of solid with surface that contains only geometric heterogeneities and thus not discussed further.

Overall, we see from fig. 19 that the nature of the FEA potential is influenced by the nature and number of all the heterogeneities present, such as the number and clustering of vacancies, and the number and clustering of hetero atoms.

4 Discussion and conclusions

? demonstrated that there can be a significant difference in the coarse-grained potentials obtained using a free-energy-averaging approach and the conventional energy-averaging procedure, and highlighted the importance of adopting the former in order to capture properly the thermodynamics of the system. In our current work, we have extended the free-energy-averaging method of Forte *et al.* to obtain coarse-grained fluid-molecule–solid-surface potentials relating to heterogeneous surfaces, and compared adsorption isotherms and fluid-density profiles obtained in adsorption simulations in which the solid substrate was treated in explicit atomistic detail with those obtained in simulations using the FEA potential. For simplicity, methane adsorbing onto graphite was used as the model system. Both chemical and geometrical heterogeneities were considered, the former implemented by modifying the solid-atom−fluid-molecule potential for randomly chosen surface atoms and the latter by introducing vacancies to the surface layer.

For the case of surface chemical heterogeneities, using the FEA potential resulted in an adsorption isotherm that was in good agreement with that obtained in the explicit-solid case. There are many other scenarios that would be of interest in relation
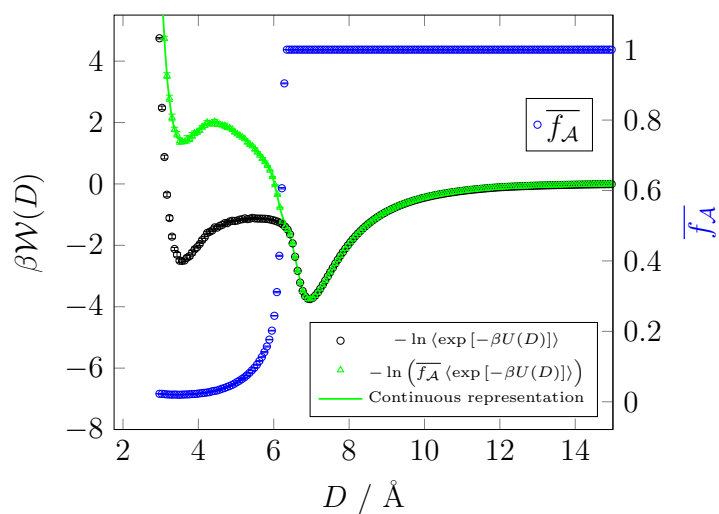
Fig. 11 The FEA potential of methane interacting with graphite of which the exposed surface (fig. 10) is geometrically heterogeneous. Black circles and green triangles represent FEA potentials obtained using eq. (7) and eq. (5), respectively. The curve indicates the continuous (fitted) representation of the FEA potential data obtained using eq. (5). Blue circles represent the fraction of the surface area available for the fluid (right vertical axis) estimated using Monte Carlo integration.
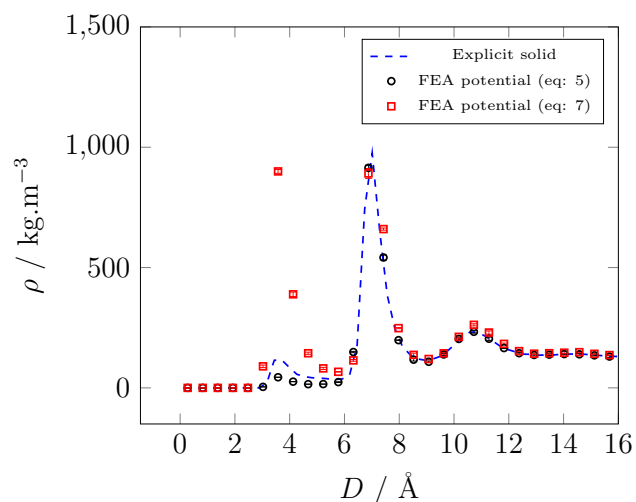

Fig. 13 The density profile (normal to the surface) of methane adsorbed on graphite of which the exposed surface (fig. 10) is geometrically heterogeneous, at a bulk pressure of 0.01279 GPa. The dashed curve corresponds to data obtained using explicit solid; the circles correspond to the profile obtained using the FEA potential (fig. 11).
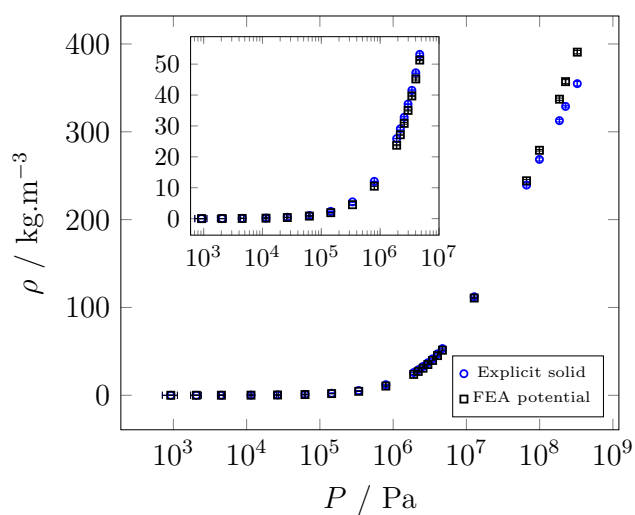

Fig. 12 Comparison of adsorption isotherms of methane on graphite of which the exposed surface (fig. 10) is geometrically heterogeneous. Blue and black squares correspond to the adsorbed fluid density values obtained using explicit solid and FEA potential, respectively.
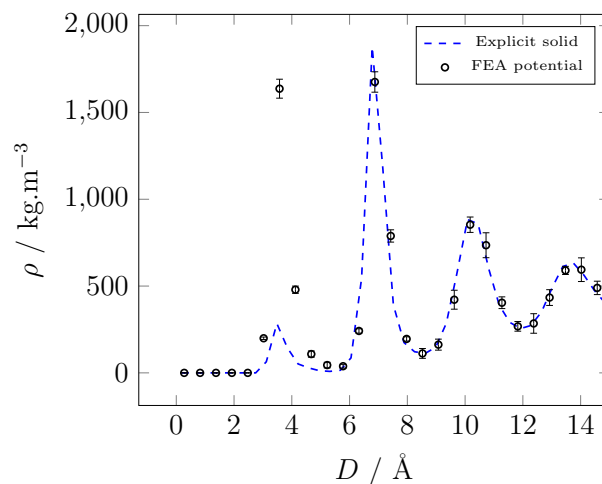

Fig. 14 The density profile (normal to the surface) of methane adsorbed on graphite of which the exposed surface (fig. 10) is geometrically heterogeneous, at a bulk pressure of 0.3265 GPa. The dashed curve corresponds to data obtained using explicit solid; the circles correspond to the profile obtained using the FEA potential (fig. 11).
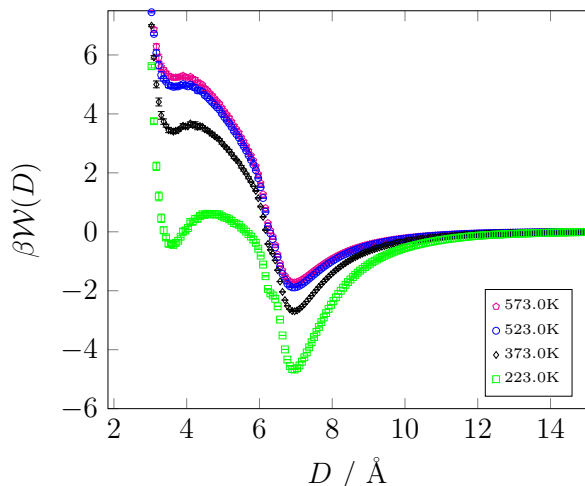
Fig. 15 Temperature dependence of FEA potentials (obtained using eq. (5)) for methane interacting with graphite of which the exposed surface (fig. 10) is geometrically heterogeneous.

future publications.

For the case of geometrical heterogeneities (exemplified here by surface vacancies) a modification to the free-energy-averaging method of **?** was implemented, allowing account to be taken of the change in the adsorbent surface brought about by the introduction of the vacancies. At low or moderate pressures, the resulting FEA potential was found to result in adsorption and fluid-density profiles in quantitative agreement with the explicit-solid case, however our work has revealed that the loss of surface detail introduces subtle inconsistencies between the explicit and coarse-grained cases when the bulk fluid pressure is sufficiently high.

Building on our findings, it is interesting once again here to refer to the recent work of Shi *et al.*, who adopted a similar framework to address the CG potential for the case of fluid interacting with solid featuring a heterogeneous surface, although with subtle differences in the methodology to that adopted in our work. These authors found that taking account of vacancies leads to CG potentials that allow for a better description of experimental adsorption isotherms. Together, the results of Shi *et al.*'s and our investigations make a strong case for the importance of adopting such a methodology.

In our *Introduction*, we discussed the wide use of the DFT framework in characterising adsorbent surfaces. Given the success of our proposed approach to developing FEA potentials, to conclude our paper we comment that it would be very interesting to see how the FEA potentials obtained using our approach could help DFT framework such as NL-DFT and QS-DFT towards characterization of adsorbent surfaces.
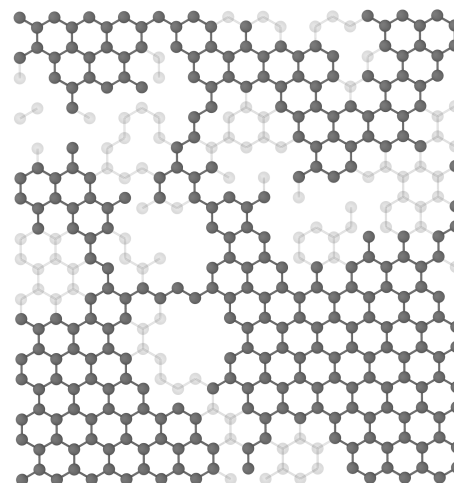

Fig. 16 Porous substrate, modelled by introducing vacancies in both the surface and second layers. Surface-layer atoms are depicted in dark grey while second-layer atoms are indicated in light grey (and are visible only when exposed by a surface-layer vacancy). Vacancies in the first layer are generated by deleting randomly chosen carbon atoms. The majority of vacancies in the second layer are located beneath those in the surface layer, generating a pitted surface.
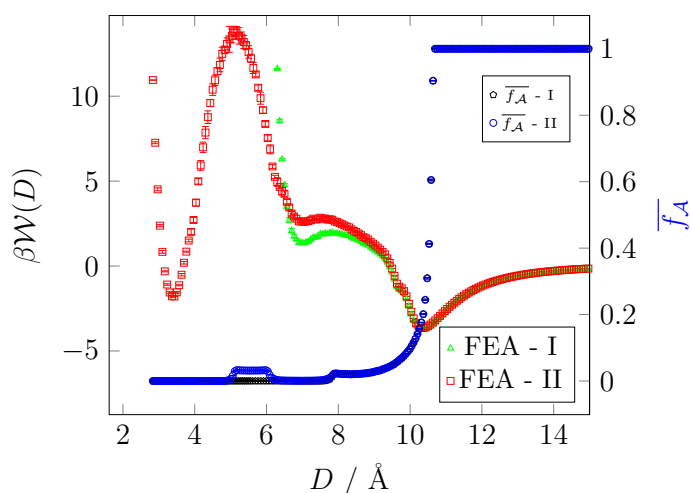

Fig. 17 FEA potentials of methane interacting with graphite. (I) the surface layer (only) contains vacancies (see fig. 10); the corresponding potential (seen also in fig. 11) is represented by green open triangles. (II) both the surface and second layers contain vacancies (see fig. 16); the corresponding potential is represented by magenta open squares. The fractional areas corresponding to these systems are indicated by black pentagons (I) and blue circles (II); note that the two coincide from $D \sim 8.5$ Å. Note that, for purposes of comparison, D is here measured for both (I)
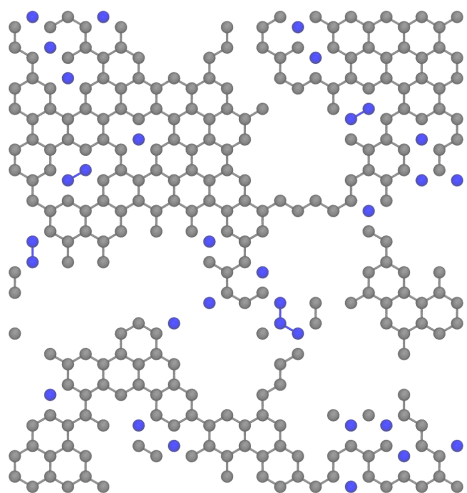
Fig. 18 Chemically and geometrically heterogeneous surface graphene layer. Those coloured in blue are (randomly selected) atoms for which the interaction with methane is modified (interaction-potential parameter values are given in table 1). Geometric heterogeneities are represented by vacancies, generated by deleting randomly chosen carbon atoms from the surface graphene layer.
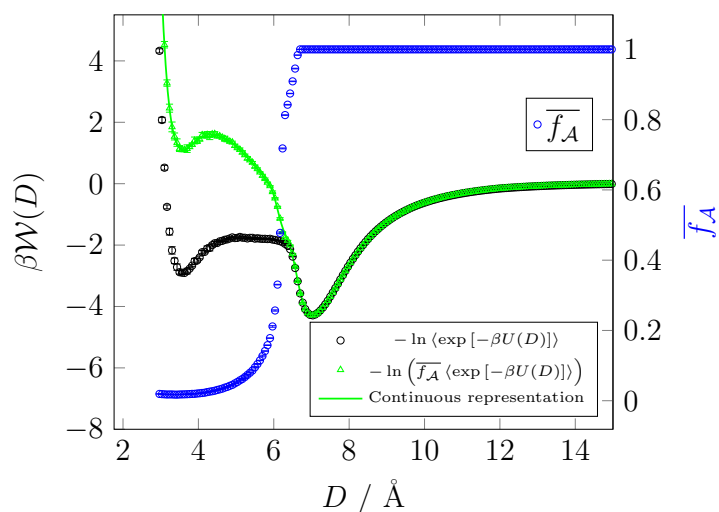

Fig. 19 The FEA potential of methane interacting with graphite of which the exposed surface (fig. 18) is both chemically and geometrically heterogeneous. Black circles and green triangles represent FEA potentials obtained using eq. (7) and eq. (5), respectively. The curve indicates the continuous (fitted) representation of the FEA potential data obtained using eq. (5). Blue circles represent the fraction of the surface area available for the fluid (right vertical axis) estimated using Monte Carlo integra-

Conflicts of interest

There are no conflicts to declare.

Acknowledgements